$^{16}O(\gamma,p)^{15}N$ reaction for $E_\gamma = 100$—400 MeV

M. J. Leitch,* J. L. Matthews, W. W. Sapp, C. P. Sargent, and S. A. Wood

*Department of Physics and Laboratory for Nuclear Science, Massachusetts Institute of Technology,
Cambridge, Massachusetts 02139*

D. J. S. Findlay† and R. O. Owens

Department of Natural Philosophy, Glasgow University, Glasgow, Scotland

B. L. Roberts

Department of Physics, Boston University, Boston, Massachusetts 02215

The differential cross section for the $^{16}O(\gamma,p)^{15}N$ process has been measured in the energy range $E_\gamma = 100$—400 MeV at laboratory angles of 45°, 90°, and 135°. The cross sections for the (γ,p) reaction leaving ^{15}N in its ground state, in its first and second excited states at $E_x \approx 5.3$ MeV, and in its third excited state at $E_x = 6.3$ MeV were extracted from the tip region of the proton spectra measured at a series of bremsstrahlung end point energies. The data are compared with calculations based on a direct, single-particle knockout mechanism and on mechanisms involving two particles in an intermediate state.

I. INTRODUCTION

Photoproton cross sections for energies above the giant dipole resonance but below the pion production threshold have previously been measured with modest energy resolution for several light- and medium-weight nuclei. Only recently have experiments achieved sufficiently good resolution to determine the cross section for the (γ,p_0) process, i.e., the reaction with the residual nucleus left in its ground state.[1,2] Cross sections for reactions populating low-lying excited states (or unresolved groups of such states) have also been obtained in a few cases.[1,3]

The primary motivation for the (γ,p) measurements lies in the large mismatch between the momentum of the outgoing proton and that of the incoming photon. The (γ,p) process will thus be one of the few reactions which are sensitive to high-momentum, short-range effects in nuclei, and it has the additional advantage of employing the relatively weak, well-understood electromagnetic probe.

The experimental results have been compared with the predictions of a direct, single-particle knockout model,[3,4] with a calculation which includes nucleon-nucleon correlations via a Jastrow model,[5] and with a theory which incorporates initial- and final-state correlations plus a representation of meson exchange currents.[6] More recently, the predictions of a self-consistent random-phase approximation theory[7] have been compared with measurements of (γ,p) and also some (p,γ) cross sections.[8] None of these calculations is able to reproduce all features of the data, and there is considerable disagreement as to the relative importance of the various possible photoreaction mechanisms.

The present experiment was undertaken in the hope that an extension of the (γ,p) measurements to higher photon energies might reveal some new features which would aid in discriminating among reaction mechanisms.

As the photon energy increases, so does the momentum mismatch, becoming two to four times the Fermi momentum at $E_\gamma \approx 400$ MeV. Since the probability of a single proton having these high momenta is very small, one would expect the direct single-particle knockout mechanism to become less important (along with at least some of the uncertainties in its description) and the reaction to show an increased sensitivity to two-nucleon processes. It is hoped that data in the $E_\gamma = 100$—400 MeV region will elucidate some of the details of these processes. Indeed, preliminary results[9] of the present experiment showed a striking departure from the trend of the (γ,p_0) cross section as a function of E_γ established at lower energies. This energy dependence suggested that a two-step, two-particle process involving the excitation and reabsorption of a virtual $\Delta(1232)$ isobar was occurring.[10]

The purpose of this paper is to report the complete experimental results for the $^{16}O(\gamma,p)$ cross sections leaving ^{15}N in its ground state and first three excited states and to compare them where possible with available calculations based on direct and two-step reaction mechanisms.

II. EXPERIMENTAL METHOD

The experiment was performed at the MIT Bates Linear Accelerator Laboratory. The $^{16}O(\gamma,p)$ cross sections were obtained from yield measurements of the top 9 MeV of the proton spectrum from a beryllium oxide target irradiated by bremsstrahlung. Photoprotons from ^9Be do not appear in this portion of the spectrum because the Q value and the recoil energy are both larger for the $^9Be(\gamma,p)$ than for the $^{16}O(\gamma,p)$ reaction.

The electron beam, analyzed to ±0.15% and energy dispersed in the vertical plane, impinged on a 245 mg cm^{-2} ($\sim$0.04 radiation length) tungsten radiator lo-

cated 10 cm upstream from the photonuclear target. The average beam current, monitored by a nonintercepting ferrite-core transformer, was typically 25 μA. The beryllium oxide target, which intercepted the entire bremsstrahlung flux, was a ceramic sheet of thickness 178 mg cm^{-2} (for $E_p < 200$ MeV) or 290 mg cm^{-2} (for $E_p > 200$ MeV). It was placed at $\pm 45°$ to the beam direction to minimize the proton energy loss in the target. The average loss (for a proton from the center of the target) was always smaller than about 1 MeV.

Protons were analyzed using the 900 MeV/c magnetic spectrometer and their momenta were determined by a focal plane drift chamber with delay-line readout[11] which was triggered by a coincidence between three plastic scintillators. Each scintillator had an area 0.25 m $\times$ 0.75 m and thickness 12.5 mm and was coupled through a twisted-strip light guide to a 75 mm diameter EMI 9821B photomultiplier tube. Iron absorber sheets placed in front of the second scintillator prevented deuterons and heavier charged particles from reaching the third detector.

The detector system, which was situated in a pit ~ 6 m below beam level, was shielded at the sides by 125 mm thick "iron curtains" and ~ 2 m thick concrete blocks. An additional three to six feet of concrete formed a roof over the pit. Massive and tightly fitting shielding between the spectrometer and the beam dump was crucial, especially for measurements at $\theta_p = 45°$.

The spectrometer's momentum bite was determined by the length of the drift chamber and was approximately 6%. The accepted solid angle, 2.9 msr, was determined by adjustable horizontal and vertical slits located between the scattering chamber and the spectrometer.

Standard fast NIM and CAMAC electronics modules were used to produce a triple coincidence trigger signal from the scintillation counters, to record the corresponding pulse heights, and to digitize the time signals from the wire chamber delay lines. The data were recorded in an event-by-event mode by a PDP 11/45 computer. Each event was characterized by a momentum channel, transverse (scattering angle) channel, and three pulse heights, together with some auxiliary diagnostic information. The data-acquisition and on-line display program is described in detail in Ref. 12.

Since the extraction of (γ,p) cross sections relies on a comparison of measured and calculated proton spectra, it was important that the momentum calibrations of the spectrometer and beam handling system were sufficiently well established to predict the position of the end point in the proton spectrum. This was especially so for those runs in which the statistical accuracy of the data was too poor to establish the end point with any precision. Fortunately, the end point at $\theta_p = 45°$ was sufficiently well defined even at the highest photon energy to determine the spectrometer calibration. The calibration procedure was based on fitting simultaneously a set of data consisting of electron elastic and inelastic scattering peaks from ^{12}C and ^{27}Al (which provided momenta up to 380 MeV/c) and ^{16}O(γ,p$_0$) end points at 45° (which provided momenta from 400 to 800 MeV/c) for electron energies between 100 and 380 MeV. The spectrometer calibration is assumed to have the form

$$p_c(B) = \sum_{m=1}^{3} b_m B^m \, ,$$

where p_c is the momentum at the center of the drift chamber and B is the spectrometer field measured by a nuclear magnetic resonance probe. The spectrometer dispersion, which has been accurately measured in electron scattering experiments, is used to obtain the calibration at other positions along the drift chamber. The calibration of the electron beam analysis system is assumed to be

$$p(I) = p_n(I)(1 + a_1 + a_2 I) \, ,$$

where $p_n(I)$ is the nominal momentum calibration obtained from electron scattering measurements and I is the analyzing magnet current. The parameters a_1, a_2, b_1, b_2, and b_3 which best fit the calibration data are determined using a χ^2 minimization program. The quality of the fits suggests that the calculated end point proton energy is reliable to ± 0.2 MeV.

Using this system, measurements of the high energy region of the proton spectrum from beryllium oxide were made at proton angles 45°, 90°, and 135° for a series of bremsstrahlung end point energies at roughly 20 MeV intervals from 100 to 380 MeV. At 90° and 135°, the small cross sections encountered at the higher energies led to a reduction of the energy range of the measurements.

III. DATA ANALYSIS AND RESULTS

A. Introduction

The basic data in this experiment are the focal plane position spectra as measured by the drift chamber. After selecting those events corresponding to protons, each position spectrum was converted to a proton energy spectrum by employing the spectrometer energy calibration. The (γ,p) cross sections leading to the ^{15}N ground and first three excited states were then extracted by fitting the measured proton spectrum with a calculated spectrum containing the (unknown) cross sections and the (known) bremsstrahlung spectrum. This procedure is described below.

B. Incident photon spectrum

In this experiment, the beryllium oxide target intercepted the entire bremsstrahlung cone as well as the electron beam. The advantages of this scheme are twofold: a large gain in intensity compared with a setup using a sweeping magnet, and the greater accuracy with which the photon spectrum may be calculated when no collimation is present. The disadvantage is that the electrons passing through the target also contribute to the proton yield. By simply removing the radiator, however, one does not directly obtain an accurate measure of the electrodisintegration contribution to the radiator-in runs; the spectrum of electrons striking the target is not the same in the radiator-in and radiator-out runs since the former are modified by the energy loss and straggling of the incident electrons in the radiator. These effects are especially im-

portant at the end point of the bremsstrahlung spectrum. In principle one could correct the radiator-out data for these effects and subtract them from the radiator-in data at each spectrometer setting to obtain the photodisintegration yield. However, to save beam time a simpler procedure was adopted, whose validity was checked as described below, in which the electrodisintegration contribution to the yield was calculated using virtual photon theory.

The effective photon flux incident on the target, with the radiator in, can be written as the sum of three components:

$$\phi^{in}(E_0,E_\gamma) = \phi_R(E_0,E_\gamma) + \phi_V^{in}(E_0,t,E_\gamma) + \phi_T^{in}(E_0,t,E_\gamma) ,$$

$$(1)$$

where ϕ_R is the bremsstrahlung spectrum produced in the radiator by electrons of mean energy E_0, ϕ_V^{in} is the virtual photon spectrum produced by electrons of mean energy E_0 which have passed through a radiator of thickness t, and ϕ_T^{in} is the bremsstrahlung produced in the target by these electrons. With the radiator out, one has

$$\phi^{out}(E_0,E_\gamma) = \phi_V^{out}(E_0,E_\gamma) + \phi_T^{out}(E_0,E_\gamma) .$$

$$(2)$$

In analyzing the $(\gamma,$p$)$ data, we have assumed that the real photon spectra ϕ_R and ϕ_T may be calculated using the formulae given in Refs. 13 and 14, in which the energy loss and straggling in the radiator (or target) are taken into account together with the energy spread of the incident electrons. The virtual photon spectrum is more uncertain, and we have therefore incorporated into ϕ_V an adjustable factor by which the transverse $E1$ spectrum given by Dalitz and Yennie[15] is multiplied. Ratios of radiator in/out data obtained at several beam energies were used to determine this factor, which in fact turned out to be 1.0 ± 0.1. Most of the $(\gamma,$p$)$ data were taken only with the radiator in and were analyzed using the composite spectrum of Eq. (1). The approximate contributions of the three components were $\phi_R \approx 65\%$, $\phi_V \approx 30\%$, and $\phi_T \approx 5\%$.

C. Measured proton spectra

The event-by-event file for each run was sorted to produce pulse height spectra for each of the scintillation counters. In these spectra the proton peaks were clearly separated from other events. Positrons and pions of the same magnetic rigidity are kinematically forbidden and particles heavier than protons are removed by the iron absorber. Pulse height constraints were applied to the spectra to select the proton events and an energy spectrum was constructed.

The energy resolution of the proton spectrum was limited principally by energy loss in the target. The effect of the 0.3% energy spread of the incident electrons was largely removed by appropriate setting of the energy dispersion of the beam on the target to match the spectrometer dispersion. Further contributions came from the spreading of the beam spot due to multiple scattering in the radiator ($\Delta E_p \approx 0.3$ MeV) and the wire spacing of the drift chamber ($\Delta E_p / E_p = 0.12\%$).

D. Calculated proton spectrum and data fitting

In order to extract the $(\gamma,$p$)$ cross sections from the experimental data, a "theoretical" proton spectrum was constructed, viz.,

$$\frac{dN_p}{dE_p} = \sum_i \left[n\Delta\Omega \left[\phi(E_0,E_\gamma)\frac{dE_\gamma}{dE_p} \right]_i \right] \frac{d\sigma_i}{d\Omega} , \qquad (3)$$

where $d\sigma_i/d\Omega$ is the cross section for reactions leading to the ith excited state in the residual nucleus. The quantities in square brackets are known: $\phi(E_0,E_\gamma)$ is the incident photon spectrum obtained from Eq. (1) or Eq. (2), n is the target density (nuclei/cm^2), and $\Delta\Omega$ is the solid angular acceptance of the spectrometer.

In calculating the proton spectrum, the result obtained from Eq. (3) was "smeared" to take account of the energy loss and straggling of the protons in the beryllium oxide target. To do this, the straggling distribution was approximated by an asymmetric triangle, allowing the integration to be performed analytically.[3] The resulting spectrum was then fitted to the data by treating the cross sections $d\sigma_i/d\Omega$ as adjustable parameters. The variation of the $d\sigma_i/d\Omega$ with photon energy over the fitted region was at first ignored and then included after cross sections at several energies had been determined and the energy dependence parametrized. This iterative procedure converged very rapidly. Provision was also made for including a constant background (determined from the region above the proton end point) in Eq. (3); in many cases this was found to be negligibly small. Finally, to allow for possible errors in the calibrations of the spectrometer and beam analysis system, the measured proton spectra could be shifted in energy in order to improve the fits. These energy shifts were generally well within the estimated calibration uncertainty.

Since the end point region of the measured proton spectra often contained relatively few events, a fitting procedure must be used which, unlike the conventional least squares method, will correctly treat channels with zero counts. Moreover, the least squares method is known to result in a consistent underfit of poor-statistics data.[16] To solve these problems, a fitting method was developed which is based on maximizing the likelihood function derived from Poisson statistics.[17,18]

The analysis procedure described above produces reliable results for the ^{16}O$(\gamma,$p$_0)^{15}$N (ground state) cross section, $d\sigma_0/d\Omega$. The cross sections for reactions leading to excited states, however, are less well determined. The ^{15}N spectrum contains a closely-spaced doublet ($\frac{1}{2}^+$, $\frac{5}{2}^+$) of levels at 5.27 and 5.30 MeV, a $\frac{3}{2}^-$ level at 6.32 MeV, and five additional positive parity states between 7 and 9 MeV excitation energy. Since it is anticipated that the $(\gamma,$p$)$ reaction would populate principally the single-hole ground ($\frac{1}{2}^-$) and 6.3 MeV ($\frac{3}{2}^-$) states, one could attempt to extract only these cross sections from the proton spectra. In some cases it was found that the fits to the data could be improved by assuming that the 5.3 MeV doublet (treated as a single state) was also populated, but the improvement was substantial in only a few instances. An example of such a fit is shown in Fig. 1. Since in the majority of cases, however, the presence of the 5.3 MeV states is not
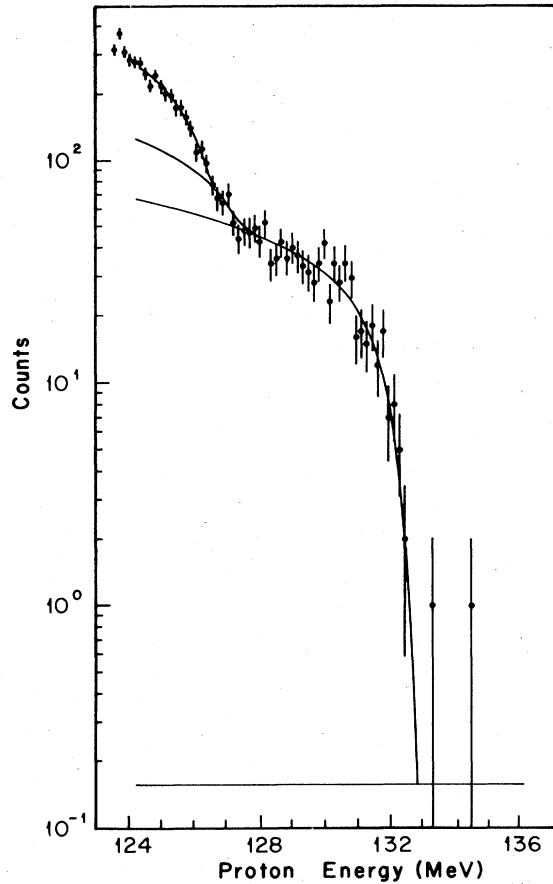
FIG. 1. Proton energy spectrum observed in the $^{16}O(\gamma,p)$ reaction at $\theta_p = 45°$ for a bremsstrahlung end point energy of 151 MeV. The solid lines represent the fit to the data (background, $d\sigma_0/d\Omega$, $d\sigma_{1,2}/d\Omega$, and $d\sigma_3/d\Omega$) as described in the text.

strongly demanded by the data, no attempt has been made to include the higher energy positive parity states whose cross sections would be even less well determined. Finally, it is noted that the result for the ground state cross section did not depend on which excited states were included in the fit; the same value within the uncertainties was obtained if Eq. (3) contained the ground state cross section alone and was fitted to the top 5 MeV of the proton spectrum.

The results of this analysis are presented in Tables I—III. Table I contains the ground state cross section, $d\sigma_0/d\Omega$, obtained by fitting the top 5 MeV of the proton spectrum, the procedure which was judged to contain the fewest uncertainties. Table II contains the cross section for excitation of the 6.3 MeV state, $d\sigma_3/d\Omega$, obtained from fitting the highest 9 MeV of the proton spectrum and assuming that only the ground and 6.3 MeV states (i.e., no positive parity states) are populated. Table III contains $d\sigma_{1,2}/d\Omega$ and $d\sigma_3/d\Omega$ for those cases in which a statistically significant result was obtainable; these cross sections are derived from fitting the highest 9 MeV of the spectrum under the assumption that the ground, 5.3, and 6.3 MeV states are populated.

E. Corrections to the data

The cross sections obtained from the fits were corrected for dead time losses. One loss arises because the electronics could not handle more than one event per beam burst. The correction, generally less than 1%, was obtained from the ratio of the total number of coincidence triggers to the number of stored events. An additional correction, typically less than 5%, is necessary for losses due to pileup in the drift chamber. This correction is derived from the

TABLE I. Laboratory cross sections for the $^{16}O(\gamma,p_0)^{15}N$ reaction.

E_γ (MeV)	θ_p 45° $d\sigma_0/d\Omega$ (nb/sr)	90° $d\sigma_0/d\Omega$ (nb/sr)	135° $d\sigma_0/d\Omega$ (nb/sr)
101.5	1119 ±23	68.2 ±2.1	17.0 ±1.7
110.7	810 ±40	31.8 ±2.0	
125.9	411 ±33	21.6 ±1.5	8.4 ±0.7
141.3		19.7 ±1.9	
151.3	103.7± 5.2	19.2 ±1.6	4.6 ±0.7
160.1		18.6 ±1.8	
166.2	53.7± 5.7		
176.2	35.3± 2.5		
181.2		12.1 ±1.0	1.97 ±0.31
201.2			1.35 ±0.19
204.4	15.0± 2.4	9.0 ±1.3	
211.2	12.3± 1.4		
221.2	12.5± 1.2	5.38±0.58	0.78 ±0.19
241.2	10.8± 1.1	4.9 ±0.8	
261.3	8.6± 1.8	2.42±0.40	0.141±0.063
281.3	7.4± 1.4	1.77±0.33	
301.4	10.9± 2.7	1.15±0.20	0.050±0.050
321.6	10.1± 1.6	0.52±0.13	
341.2	9.4± 1.3	0.17±0.10	
361.8	6.5± 1.3		
382.0	5.4± 0.9		

TABLE II. Laboratory cross sections for the $^{16}O(\gamma,p_3)^{15}N$ reaction assuming that only the ground and third (6.32 MeV) excited states of ^{15}N are populated.

E_γ (MeV) \ θ_p	45° $d\sigma_3/d\Omega$ (nb/sr)	90° $d\sigma_3/d\Omega$ (nb/sr)	135° $d\sigma_3/d\Omega$ (nb/sr)
101.5	4530 ±290		
110.7	3670 ±860	253 ±19	
125.9		166 ±42	40.3±5.5
141.3		204 ±48	
151.3	744 ± 56	125 ±10	38.3±4.2
160.1		125 ±16	
166.2	488 ± 45		
176.2	344 ± 22		
181.2		84.9 ± 5.6	8.1±1.8
201.2			3.9±1.0
204.4	152 ± 28	74 ± 11	
211.2	182 ± 12		
221.2	144 ± 12	24.3 ± 3.7	2.3±1.1
241.2	128 ± 8	15.8 ± 2.8	
261.3	142 ± 10	9.3 ± 2.3	
281.3	85 ± 9	4.6 ± 1.8	
301.4	74 ± 16	3.8 ± 1.3	
321.6	44 ± 9	0.59± 0.64	
341.2	27.4± 5.9	0.67± 0.48	
361.8	18.6± 5.2		
382.0	14.3± 4.1		

fraction of events for which an ambiguous result is obtained from the analysis of the drift chamber information. Finally, the cross sections were corrected for losses due to nuclear interactions of the protons in the iron absorbers and the plastic scintillators, an effect almost entirely due to the iron. The correction was estimated from reaction cross sections given by Measday and Richard-Serre[19] which are nearly constant in the relevant proton energy range. Since the absorber thickness used increased with energy, the correction varied from 5% at $E_\gamma = 100$ MeV to 29% at 380 MeV.

F. Results

The subsequent discussion of the results of this experiment is based mainly on the assumption that only the ground ($\frac{1}{2}^-$) and 6.3 MeV ($\frac{3}{2}^-$) states are populated. As seen from Table III, there is generally little evidence that

TABLE III. Laboratory cross sections for the $^{16}O(\gamma,p_{1,2})^{15}N$ and $^{16}O(\gamma,p_3)^{15}N$ reactions, assuming that the ground, first-plus-second ($\sim$5.3 MeV), and third (6.32 MeV) excited states of ^{15}N are populated.

E_γ (MeV) \ θ_p	45° $d\sigma_{1,2}/d\Omega$ (nb/sr)	45° $d\sigma_3/d\Omega$ (nb/sr)	90° $d\sigma_{1,2}/d\Omega$ (nb/sr)	90° $d\sigma_3/d\Omega$ (nb/sr)	135° $d\sigma_{1,2}/d\Omega$ (nb/sr)	135° $d\sigma_3/d\Omega$ (nb/sr)
101.5	620±240	3350± 530				
110.7	570±420	1930±1280	65±23	143±43		
125.9			44±18	22±63	11.0±5.8	23±11
141.3			41±21	73±79		
151.3	193± 61	476± 46	24±14	90±22	0.6±6.1	42± 9
160.1			10±15	115±29		
166.2	124± 38	319± 62				
176.2	108± 22	193± 35				
181.2			10± 8	71±12	1.1±2.8	6.6± 4.2
204.4			26±13	42±24		
211.2	27± 11	144± 20				
221.2	12± 10	127± 18				
241.2	1± 8	120± 15				
261.3	18± 11	117± 17				
281.3	10± 10	71± 17				
321.6	2± 13	42± 20				
341.2	6± 9	19± 14				
361.8	12± 9	3± 13				

the cross section leading to the 5.3 MeV positive parity states is a significant fraction of that for excitation of the 6.3 MeV state. The $^{16}O(\gamma,p_0)$ and (γ,p_3) differential cross sections at proton angles 45°, 90°, and 135° are given as a function of photon energy in Tables I and II and in Figs. 2 and 3. The errors quoted are the statistical uncertainties combined with an energy-dependent error which varies from 1.7% for $E_\gamma \leq 151$ MeV to 9% at $E_\gamma = 380$ MeV, due to the uncertainty in the correction for nuclear interactions of the protons in the plastic scintillators and iron absorbers. In addition, there are systematic uncertainties of $\sim 4\%$ and $\sim 3\%$, arising from uncertainties in the incident photon flux and the dead time correction, respectively.
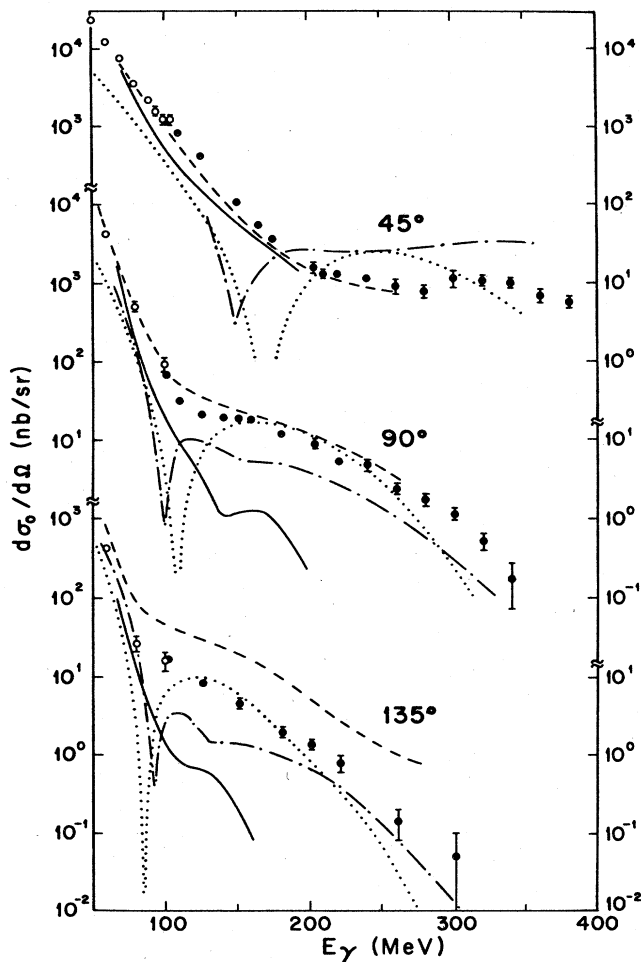
FIG. 2. Laboratory cross section for the $^{16}O(\gamma,p_0)^{15}N$ reaction at $\theta_p = 45°$, 90°, and 135° as a function of incident photon energy. The open circles are the data of Findlay and Owens (Ref. 2); the solid circles are the results of the present experiment. The curves represent the theoretical calculations discussed in the text: Dotted curves—quasi-deuteron model of Schoch (Refs. 23 and 24); dashed curves—model of Gari and Hebach which includes meson exchange effects (Ref. 22); dot-dashed curves—model of Londergan and Nixon which includes Δ-resonance excitation (Ref. 27); solid curves—QFK calculation of Boffi *et al.* (Ref. 4), with the bound state potential of Ref. 37 and the continuum state optical potential of Ref. 38.
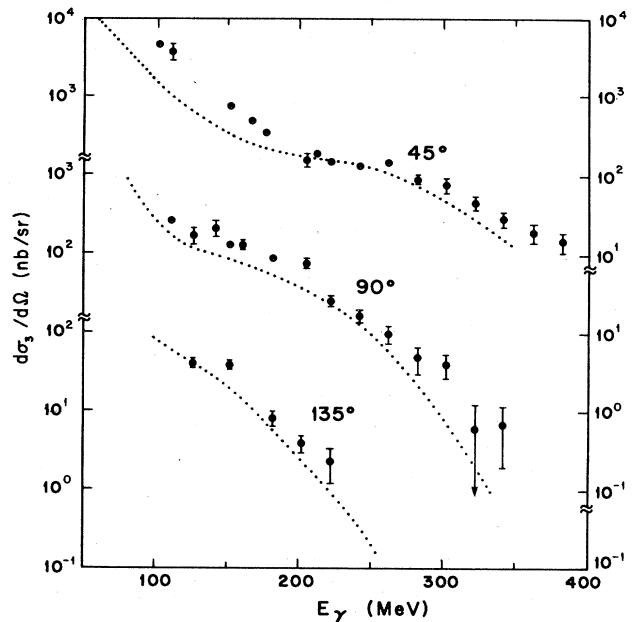
FIG. 3. Laboratory cross section for the $^{16}O(\gamma,p_3)^{15}N$ reaction (obtained assuming that only the ground and 6.32 MeV states of ^{15}N are populated) at $\theta_p = 45°$, 90°, and 135° as a function of photon energy. The curves represent the quasi-deuteron model calculation of Schoch (Refs. 23 and 24).

The only data available for comparison with the present results are those of Findlay and Owens[2] at $E_\gamma \leq 100$ MeV, which are also shown in Fig. 2. The agreement is good.

IV. DISCUSSION

This section begins with a qualitative description of the main features of the experimental results. The existing theoretical treatments of exclusive (γ,N) reactions at intermediate energies are then summarized and the present data are examined to determine the extent to which they can resolve uncertainties in the interpretation of the lower-energy measurements.

Compared with the previously available exclusive (γ,N) data, the new results over a wider photon energy range do exhibit qualitatively different features. As seen in Figs. 2 and 3, the cross section, which decreases rapidly with increasing photon energy below 100 MeV, becomes less steeply falling at higher energies. This behavior suggests that the mechanism principally responsible for the (γ,p) reaction changes across the 100—250 MeV region. The change in slope occurs at a different photon energy and to a different extent at each proton angle. However, in terms of the momentum mismatch $q = |q_N - q_\gamma|$ between the outgoing nucleon's momentum q_N and that of the incident photon q_γ, the change occurs at approximately the same momentum, $q \approx 500$ MeV/c. The cross sections leading to different states in the residual nucleus show qualitatively similar trends, although the ratios of the cross sections to different states are by no means constant. The ratios of the (γ,p_3) and (γ,p_0) cross sections exhibit a

systematic variation with photon energy and proton angle as shown in Fig. 4, but the $(\gamma,p_{1,2})$ cross section has more nearly the same shape as that for the ground state protons.

In the theoretical work on exclusive (γ,N) reactions quite different views have been expressed on the relative importance of the contributing reaction mechanisms. In particular this is the case for the direct knockout mechanism in which the photon interacts with a single quasi-free nucleon. Experiments on the (γ,n) reaction[20,21] for photon energies $E_\gamma \leq 160$ MeV show that the cross section is similar to that for the (γ,p) reaction, although somewhat smaller in magnitude and less strongly forward peaked. Since the photon couples only relatively weakly to the neutron through its magnetic moment, it would seem unlikely that quasi-free knockout (QFK) can be responsible for the observed (γ,n) cross section. Several authors[6,7,22,23] have concluded that the QFK mechanism makes little contribution and have attempted to explain the (γ,N) results in terms of models which involve more than one nucleon in the absorption process. The relative ease with which a large momentum mismatch can be obtained when several nucleons are involved suggests that such mechanisms will indeed be important.
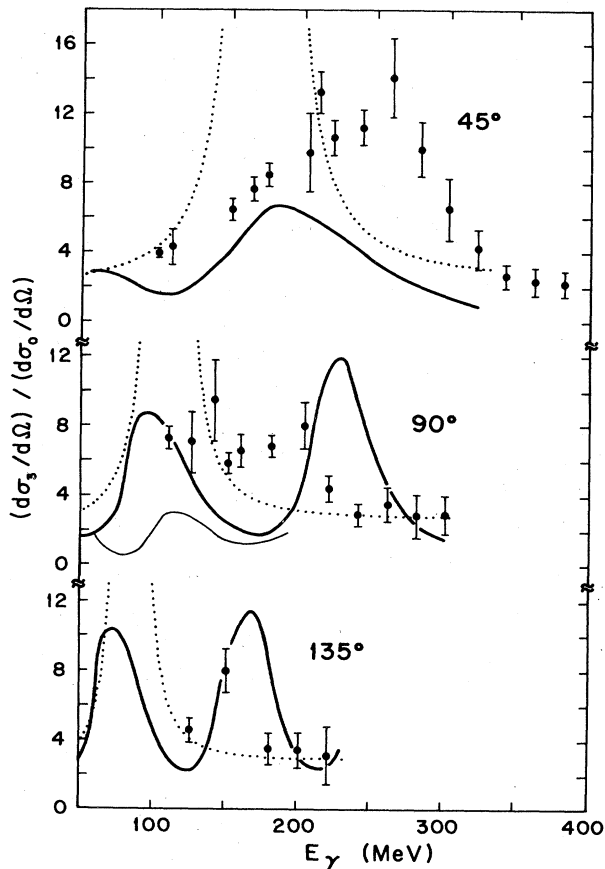
FIG. 4. Ratio of cross sections for the $^{16}O(\gamma,p_3)^{15}N$ and $^{16}O(\gamma,p_0)^{15}N$ reactions at $\theta_p = 45°$, 90°, and 135° as a function of photon energy. The light (Ref. 29) and dark (Ref. 12) solid curves are both based on the QFK mechanism, as discussed in the text. The dotted curves represent the quasi-deuteron model calculations of Schoch (Refs. 23 and 24).

A. Two-nucleon mechanisms

At a phenomenological level the quasi-deuteron model has provided a very successful description of a wide range of data on inclusive photoreactions above the giant resonance. Schoch[23] has modified this model for application to exclusive (γ,N) reactions to account for one of the two struck nucleons remaining in the final nucleus. This approach builds in the similarity of the (γ,p) and (γ,n) cross sections as observed experimentally. A detailed comparison with the measured angular distributions, for example, is necessary to test whether the assumed absorption by a neutron-proton pair is responsible for a major part of the cross sections. In this picture the momentum mismatch is made up of three contributions, the initial momentum of the knocked-out nucleon and both the initial and final momenta of the other nucleon. Schoch's treatment combines these latter two contributions into a term $F(q_R)$, which he suggests can be identified approximately with the form factor of the residual nucleus. The predicted angular distributions and cross sections to different final states are determined to a large extent by the shape of the relevant form factor, F. Figures 2 and 3 show the comparison of a quasi-deuteron calculation[24] based on the formalism of Ref. 23 with the data for the (γ,p_0) and (γ,p_3) reactions.

The strong variations in the predicted E_γ dependence reflect the diffraction structure in $F(q_R)$, and the predictions do account for the general trends of the data at the three measured angles, although it is known[25] that at very forward angles the quasi-deuteron calculation does not work well. The deep minima in the calculated ground state cross section probably result from the approximations adopted, in particular the plane wave treatment of the outgoing nucleon. The ratio of the (γ,p_0) and (γ,p_3) cross sections is shown in Fig. 4 together with the result of the quasi-deuteron calculation,[24] which is determined by the different behavior of the form factors for the two residual states. If allowance is made for the unrealistic minimum in $F(q_R)$ for the ground state, the prediction does have the right general trend, although the calculated peak in the ratio occurs at too low a photon energy. [The calculation works rather better for the $(\gamma,n_3)/(\gamma,n_0)$ ratio at lower energies.[23]]

A much more detailed calculation of the $^{16}O(\gamma,N)$ reactions has been carried out by Gari and Hebach.[22] The extensive results obtained offer the prospect of separating the contributing mechanisms since their relative importance is found to vary considerably with photon energy and nucleon angle. In this calculation the terms corresponding to an effective two-body interaction of the photon are not treated individually but are included by using their relation to the residual nucleon-nucleon interaction. This procedure takes into account the contributions due to meson exchange and initial- and final-state correlations. Gari and Hebach emphasize the importance of these terms, which are required by gauge invariance but which are omitted in many calculations. In their results the gauge terms do dominate over most of the region studied, the contribution from QFK being small. Unfortunately no attempt was made to examine the sensitivity of the results to the parametrizations which were employed to

describe either the residual interaction or the potentials for bound and continuum states. The unrealistically deep potential chosen in order to maintain orthogonality when evaluating the continuum wave functions certainly depresses the QFK contribution, and it has been argued[2] that this is not the best compromise. A comparison between the calculations of Ref. 22 and the (γ, p_0) data is shown in Fig. 2. The calculations do reproduce the observed change in slope of the cross sections; in this case it is caused by the interference between the meson exchange and QFK contributions, which is constructive at low photon energies but becomes destructive at higher energies due to the location of a zero in the bound state momentum wave function. At 45° the calculated curve including Δ-resonance contributions agrees well with the data but the agreement is not as good at the other angles. It is not clear why the Δ contribution was not included at 90° since it makes a large contribution in the 0°—60° range for which it was calculated. For angles larger than 105°, Gari and Hebach comment[22] that "the cross sections are too small for reliable prediction," and have suggested[26] that there might be cancellations arising from less important mechanisms which were not included in their calculation. In its present form the calculation of Ref. 22 will not explain the different E_γ dependence observed for the (γ, p_3) cross section since the bound state potential used has no spin-orbit part.

A calculation, which is basically rather similar to that of Gari and Hebach,[22] has been carried out by Cavinato *et al.*[7] with results which are in qualitative agreement with those of Ref. 22. Since these calculations only extend up to $E_\gamma = 80$ MeV, they are not included in Figs. 2 and 3.

Isobar excitation in an intermediate state in $^{16}O(\gamma, N)$ reactions has been treated in a detailed microscopic way by Londergan and Nixon[27] in order to determine the importance of this particular two-body contribution. Their calculation, which contains only the QFK term in addition to Δ excitation, is claimed to be "parameter-free" since the basic coupling constants are taken from experiment. Several effects such as center-of-mass corrections, ρ-meson exchange, and modifications of the Δ width were examined, but none altered the qualitative features of the results, which are shown in Fig. 2. Again the trend of the (γ, p_0) cross sections, in particular the change in slope in the 100—200 MeV region, is reproduced quite well at all three angles, apart from some structure in the calculated results caused by the use of approximate distorted wave functions for the outgoing protons. In this treatment the change in slope is interpreted as the transition between two regions in which different mechanisms dominate, QFK at lower energies and isobar production at higher energies. The calculation of Londergan and Nixon, like that of Gari and Hebach,[22] cannot produce any significant difference between the (γ, p_3) and (γ, p_0) cross sections since the spin-orbit part of the nuclear potential is omitted.

Although the calculations[22,23,27] described above, which were carried out to investigate the two-body mechanisms in exclusive (γ, N) reactions, achieve qualitative agreement with the present data, they do not clarify the position re-

garding the (γ, p) reaction mechanism. The theoretical results show a wide variation in the importance ascribed to different mechanisms. For example, in the calculation of Londergan and Nixon[27] the onset of Δ excitation is completely responsible for the trend of the results at higher energies, whereas this process is of much less importance according to Gari and Hebach.[22] The change in slope of the cross section is also explained differently in the three treatments, although in each case it is related to the structure in the bound state momentum wave functions of the nucleons which participate in the interaction. The basis of the treatment of Londergan and Nixon has been strongly criticized by Gari and Hebach, whose own conclusions are also not beyond question in view of their failure to investigate the effects of the somewhat arbitrary parametrizations employed.

B. Quasi-free knockout mechanism

With the exception of Londergan and Nixon[27] the investigators of two-nucleon absorption mechanisms in (γ, N) reactions have concluded that the QFK mechanism alone would fall far short of the data at all energies. However, this may be an unjustified conclusion. Boffi *et al.*[4] have shown that the QFK cross section for the (γ, p) reaction is very sensitive to the choice of initial and final state potentials (as expected) and that within the range of acceptable potentials it is possible to account for the data up to $E_\gamma \approx 100$ MeV using nuclear wave functions which are also consistent with (e,e′p) experiments. One of the set of calculations carried out by Boffi *et al.* for the $^{16}O(\gamma, p_0)$ reaction is shown in Fig. 2. This result is consistent with an earlier conclusion of the present authors[28] that, assuming only QFK contributes, a momentum distribution which is both self-consistent and in agreement with that obtained from the (e,e′p) data can be extracted from the lower energy (γ, p_0) measurements. In the QFK picture, marked differences between the (γ, p_0) and (γ, p_3) cross sections are expected, reflecting the differences between the initial bound state momentum distributions for $p_{1/2}$ and $p_{3/2}$ protons. It is anticipated that the (γ, p_3) to (γ, p_0) cross section ratios will be sensitive to the choice of initial and final state potentials; this is confirmed by the two distorted-wave QFK calculations[12,29] shown in Fig. 4. Their agreement with the data, while not good, is not inferior to that obtained by Schoch in the quasi-deuteron framework, even after allowing for the unrealistic minima in the latter, basically plane-wave, calculation.

The objections which have been raised to these QFK calculations are twofold: First, the calculations have not used orthogonal wave functions for the bound and continuum states, and second, a calculation for the (γ, p) reaction which fails entirely to explain the (γ, n) data must be inherently suspect. Several papers[30−32] have considered the first point and either estimated the errors or proposed solutions. Boffi *et al.*[30,31,33] justify a simple correction to remove the effects, which they find to be relatively small, due to the use of different bound and continuum state potentials. To assess the validity of the second objection other possible contributions to the (γ, n) cross section must be evaluated. One contribution which would transfer

strength from the (γ,p) to the (γ,n) reaction following an initial quasi-free interaction is charge exchange by the outgoing proton. Cotanch[34] has estimated the strength of this process at lower photon energies and his results suggest that it is important and should be included in calculations for $E_\gamma > 60$ MeV. The results of Gari and Hebach[22] also provide a hint that charge exchange will be a large effect since a major part of the (γ,n) cross section in their calculation for $E_\gamma < 200$ MeV arises from the correlation terms which include final state interactions. The second additional contribution to the (γ,n) process is the so-called recoil term in which the photon interacts coherently with ($A - 1$) nucleons leading to the emission of the remaining neutron or proton. This contribution has been investigated recently,[21,31,33,35,36] and it is found to be large, especially at backward angles. With these results in mind it no longer seems justifiable to conclude from the similarity of the (γ,n) and (γ,p) cross sections that the QFK mechanism is unimportant, although equally it seems very unlikely that it is dominant.

V. CONCLUSIONS

The (γ,p) data reported here considerably extend the range covered by the previous experiments, but, despite the changes in the energy dependence of the cross sections which were observed, comparison with the available theoretical work still does not allow any definitive conclusion about the reaction mechanisms. The fault lies both with the data and the calculations, neither of which are sufficiently comprehensive.

It is now clear that no single mechanism dominates the (γ,N) process over a large part of the whole energy and angular range, although it is at least fairly well established that two-nucleon mechanisms provide the major contribution for $E_\gamma > 100$ MeV. Only a detailed theoretical treatment, which includes all likely mechanisms and investigates the effects of the parametrizations employed, will

provide further understanding of the extent to which the specific characteristics of these mechanisms can be identified in the data. In the approach of Gari and Hebach, for example, one must question both the appropriateness of the chosen continuum potential and whether the residual interaction used has a sufficiently realistic form. The quasi-deuteron calculation of Schoch is interesting since it suggests that many of the observable features of the two-nucleon (γ,N) mechanisms do not depend on the details of the strong N-N interaction but are determined by the ability of the residual nucleus to accept momentum. It is hardly surprising that the attempt to parametrize the process of photon absorption by a strongly interacting nucleon pair in terms of the deuteron photodisintegration cross section is not entirely successful. Indeed, it would be disappointing if it were so since one aim of the experiments is to probe these strong interactions.

The most obvious deficiency of the experimental $^{16}O(\gamma,p)$ data is the lack of complete angular distributions above $E_\gamma = 100$ MeV. The measurements reported here were made at three angles only and are not adequate as a test of calculations which predict angular distributions exhibiting distinctive structure which varies quite rapidly with photon energy (see, e.g., Ref. 22). This deficiency should soon be partially remedied; one complete angular distribution has now been obtained[18] and further measurements are planned.

ACKNOWLEDGMENTS

*Present address: Los Alamos National Laboratory, Los Alamos, NM 87545.

†Present address: Atomic Energy Research Establishment, Harwell, Oxfordshire, England.

[1]J. L. Matthews, D. J. S. Findlay, S. N. Gardiner, and R. O. Owens, Nucl. Phys. A267, 51 (1976).

[2]D. J. S. Findlay and R. O. Owens, Nucl. Phys. A279, 385 (1977).

[3]D. J. Gibson, Ph.D. thesis, Glasgow University, 1979 (unpublished).

[4]S. Boffi, C. Giusti, and F. D. Pacati, Nucl. Phys. A359, 91 (1981).

[5]W. Weise and M. G. Huber, Nucl. Phys. A162, 330 (1971). See also Ref. 1.

[6]H. Hebach, A. Wortberg, and M. Gari, Nucl. Phys. A267, 425 (1976).

[7]M. Cavinato, M. Marangoni, P. L. Ottaviani, and A. M. Saruis, Nucl. Phys. A373, 445 (1982); M. Cavinato, M. Marangoni, and A. M. Saruis, Nuovo Cimento 76A, 197 (1983); Nucl. Phys. A422, 237 (1984); A422, 273 (1984).

[8]M. Anghinolfi et al., Nucl. Phys. A399, 66 (1983); Phys. Rev. C 28, 1005 (1983).

[9]J. L. Matthews et al., Phys. Rev. Lett. 38, 8 (1977).

[10]J. T. Londergan, G. D. Nixon, and G. E. Walker, Phys. Lett. 65B, 427 (1976).

[11]W. Bertozzi et al., Nucl. Instrum. Methods 141, 457 (1977); 162, 211 (1979).

[12]M. J. Leitch, Ph.D. thesis, Massachusetts Institute of Technology, 1979 (unpublished).

[13]J. L. Matthews and R. O. Owens, Nucl. Instrum. Methods 111, 157 (1973).

[14]J. L. Matthews, D. J. S. Findlay, and R. O. Owens, Nucl. Instrum. Methods 180, 573 (1981).

[15]R. H. Dalitz and D. R. Yennie, Phys. Rev. 105, 1598 (1957); W. C. Barber and T. Wiedling, Nucl. Phys. 18, 575 (1960).

[16]P. R. Bevington, Data Reduction and Error Analysis for the Physical Sciences (McGraw-Hill, New York, 1969), p. 248.

[17]S. A. Wood, Ph.D. thesis, Massachusetts Institute of Technology, 1983 (unpublished).

[18]R. S. Turley, Ph.D. thesis, Massachusetts Institute of Technol-

ogy, 1984 (unpublished).

[19]D. F. Measday and C. Richard-Serre, CERN Report 69-17, 1969 (unpublished).

[20]H. Göringer and B. Schoch, Phys. Lett. **97B**, 41 (1980); B. Schoch and H. Göringer, *ibid*. **109B**, 11 (1982); H. Göringer, B. Schoch, and G. Lührs, Nucl. Phys. **A384**, 414 (1982).

[21]M. R. Sené *et al.*, Phys. Rev. Lett. **50**, 1831 (1983); M. R. Sené *et al.*, Nucl. Phys. (to be published).

[22]M. Gari and H. Hebach, Phys. Rep. **72**, 1 (1981).

[23]B. Schoch, Phys. Rev. Lett. **41**, 80 (1978); Habilitationsschrift, Universität Mainz, 1980 (unpublished).

[24]M. R. Sené, Ph.D. thesis, University of Edinburgh, 1982 (unpublished).

[25]B. Schoch *et al.*, Phys. Rev. C **22**, 2630 (1980).

[26]H. Hebach, private communication.

[27]J. T. Londergan and G. D. Nixon, Phys. Rev. C **19**, 998 (1979).

[28]D. J. S. Findlay and R. O. Owens, Phys. Rev. Lett. **37**, 674 (1976); Nucl. Phys. **A292**, 53 (1977); D. J. S. Findlay *et al.*, Phys. Lett. **74B**, 305 (1978); J. L. Matthews, in *Momentum Wave Functions—1982*, Proceedings of the Second Workshop on Momentum Wave Functions in Atomic, Molecular, and Nuclear Systems, Adelaide, South Australia, AIP Conf. Proc.

No. 86, edited by E. Weigold (AIP, New York, 1982), p. 57.

[29]S. Boffi, C. Giusti, and F. D. Pacati, in Proceedings of the 3rd International Conference on Nuclear Reaction Mechanisms, Varenna, 1982, edited by E. Gadioli (University of Milano, Milano, 1982).

[30]S. Boffi *et al.*, Nucl. Phys. **A379**, 509 (1982).

[31]S. Boffi, R. Cenni, C. Giusti, and F. D. Pacati, Nucl. Phys. **A420**, 138 (1984).

[32]C. Ciofi degli Atti, M. M. Giannini, and G. Salme, Nuovo Cimento **76A**, 225 (1983); F. Cannata, J. P. Dedonder, and S. A. Gurwitz, *ibid*. **76A**, 478 (1983); Q. Haider and J. T. Londergan, Phys. Rev. C **23**, 19 (1981); L. S. Celenza and C. M. Shakin, *ibid*. **20**, 385 (1979); J. V. Noble, *ibid*. **17**, 2151 (1978); J. M. Eisenberg, J. V. Noble, and H. J. Weber, *ibid*. **19**, 276 (1979).

[33]S. Boffi, Nuovo Cimento **76A**, 186 (1983).

[34]S. R. Cotanch, Phys. Lett. **76B**, 19 (1978).

[35]S. Boffi, C. Giusti, F. D. Pacati, and M. Rosa-Clot, Nuovo Cimento **76A**, 685 (1983).

[36]R. Cenni and G. A. Rottigni, Lett. Nuovo Cimento **15**, 574 (1976).

[37]J. W. Negele, Phys. Rev. C **1**, 1260 (1970).

[38]D. F. Jackson and I. Abdul-Jalil, J. Phys. G **5**, 1699 (1979).